ELSEVIER

Journal of Biomechanics 35 (2002) 803–811

JOURNAL OF BIOMECHANICS

www.elsevier.com/locate/jbiomech
www.JBiomech.com

Mechanical behavior of coronary stents investigated through the finite element method

Francesco Migliavacca[a,*], Lorenza Petrini[b], Maurizio Colombo[a], Ferdinando Auricchio[b], Riccardo Pietrabissa[a]

[a] *Laboratory of Biological Structure Mechanics, Dipartimento di Bioingegneria, Politecnico di Milano, Piazza Leonardo da Vinci, 32, Milano 20133, Italy*

[b] *Dipartimento di Meccanica Strutturale, Università degli Studi di Pavia, Italy*

Accepted 5 February 2002

Abstract

Intravascular stents are small tube-like structures expanded into stenotic arteries to restore blood flow perfusion to the downstream tissues. The stent is mounted on a balloon catheter and delivered to the site of blockage. When the balloon is inflated, the stent expands and is pressed against the inner wall of the coronary artery. After the balloon is deflated and removed, the stent remains in place, keeping the artery open. Hence, the stent expansion defines the effectiveness of the surgical procedure: it depends on the stent geometry, it includes large displacements and deformations and material non-linearity.

In this paper, the finite element method is applied (i) to understand the effects of different geometrical parameters (thickness, metal-to-artery surface ratio, longitudinal and radial cut lengths) of a typical diamond-shaped coronary stent on the device mechanical performance, (ii) to compare the response of different actual stent models when loaded by internal pressure and (iii) to collect suggestions for optimizing the device shape and performance.

The stent expansion and partial recoil under balloon inflation and deflation were simulated. Results showed the influence of the geometry on the stent behavior: a stent with a low metal-to-artery surface ratio has a higher radial and longitudinal recoil, but a lower dogboning. The thickness influences the stent performance in terms of foreshortening, longitudinal recoil and dogboning.

In conclusion, a finite element analysis similar to the one herewith proposed could help in designing new stents or analyzing actual stents to ensure ideal expansion and structural integrity, substituting in vitro experiments often difficult and unpractical.

Keywords: Coronary stent; Finite element method; Numerical simulations; Mechanical response; Mathematical model

1. Introduction

Intravascular stents are small tube-like structures placed into stenotic arteries to restore blood flow perfusion to the downstream tissues. The first implanted stent was described by Dotter (1969) to treat arterial shrinkage, but the clinical routine implantation began in the 1990s to improve the limitations of balloon angioplasty, such as restenosis and abrupt closure (Dangas and Fuster, 1996; Gottsauner-Wolf et al., 1996). If compared to angioplasty, higher efficiency of stents is supported by randomized trials and clinical studies (Fischman et al., 1994; Serruys et al., 1994; Versaci et al., 1997). Nevertheless, problems and difficulties remain, such as migrations, collapses, cloth formations or positioning difficulties (Bjarnason et al., 1993; Wong et al., 1996; Rosenfield et al., 1997).

Different typologies of stents are available on the market and the importance for the operator to know the different physical properties of the stent selected to treat a specific lesion is recognized. Up to now, apart from the manufacturer claims, available useful information come from some experimental comparative studies (Rieu et al., 1999; Dyet et al., 2000; Ormiston et al., 2000; Barragan et al., 2000). Only recently, numerical analyses with finite element method (FEM) have been proposed as an alternative approach to investigate mechanical properties of intravascular stents.

*Corresponding author. Tel.: +39-02-2399-4283; fax: +39-02-2399-4286.

E-mail address: migliavacca@biomed.polimi.it (F. Migliavacca).

0021-9290/02/$ - see front matter
PII: S0021-9290(02)00033-7

Although FEM is nowadays a methodology well known and widely used in many engineering fields (mechanical, structural, aeronautical, etc.), it is worthwhile remembering that the reliability of the results clearly depends on the assumptions and hypotheses adopted in the analysis. Indeed, the stent expansion includes geometric and material non-linearities, which are difficult to be properly simulated. As far as we know, apart from in vitro fluid dynamics studies on intravascular stent (Peacock et al., 1995; Fabregues et al., 1998), structural FEM analyses were used by Dumoulin and Cochelin (2000) to evaluate and characterize some mechanical properties of balloon-expandable stent, by Etave et al. (2001) to compare the performance of two different types of stent, by Auricchio et al. (2001) who realized a 3D study of the stent–artery interaction during stent deployment, by Rogers et al. (1999) who studied a 2D balloon–artery interaction, and by Oh et al. (1994) who exploited FEM to analyze the stress state of atherosclerotic artery during balloon angioplasty. Examples of the advantages in the use of FEM model in predicting the mechanical behavior of stents and balloons are reported also by Whitcher (1997).

Actually, although intravascular stents are nowadays routinely and successfully used, research and developments are still necessary, in particular to improve the design and to reduce the long-term failure.

The purpose of this work is to show how the FEM can be used in the optimization of the design of coronary intravascular stent. In particular, the FEM is herewith applied to investigate the effects of different geometrical features on the mechanical performance of a widely adopted stent and to compare the response of different stent models.

To reach these goals, the study was organized as described in the following:

- A 3D FEM model of a typical diamond-shaped q(DS) intravascular stent (Palmaz-Schatz)[1] was developed to investigate the effects of different geometrical features (such as thickness, longitudinal and radial length of cuts) on the mechanical behavior of the stent. The stent performance was evaluated in terms of radial recoil, longitudinal qrecoil, foreshortening, and dogboning. On the basis of some preliminary results, a modification of this geometry is also proposed to minimize the dogboning effect.
- Two additional types of stent similar in the strut design to those available on the market, and comparable in terms of dimension (length, diameter, thickness of the strut) to the typical DS stent were studied.

[1] Johnson & Johnson, Interventional System, Warren, NJ, USA.

2. Materials and methods

2.1. Diamond-shaped stent

2.1.1. 3D geometrical model

A 3D model of a typical DS intravascular stent, obtained, for example, from a cylinder worked with laser technology is depicted in Fig. 1 in its unexpanded configuration. It is assumed to be a tube with rectangular slots on its surface. The stent has a length L of 16 mm, an outer diameter D of 1.2 mm, a thickness s of 0.1 mm, five slots in the longitudinal direction and 12 slots in the circumferential direction with length l of 2.88 mm, and a metal/artery index of 0.3 (model DS). The metal/artery index is defined as α_P/α_V, where α_V is the angle described by the slot and α_P is the angle described by the metal in the cross section in the unexpanded configuration (Fig. 1). It is interesting to observe that the metal/artery index α_P/α_V can be related to the actual metal surface (m) in contact with the arterial wall surface (a): model DS has a ratio m/a of 0.329.

A parametric analysis was performed by varying in model DS the slot length (l), the stent thickness (s) and the metal/artery index (α_P/α_V) alternatively. In particular, 8 different models were compared with model DS, having the following values of the parameters:

- an α_P/α_V ratio of 0.02 (model $DS_{\alpha 1}$), of 0.60 (model $DS_{\alpha 2}$), of 1.00 (model $DS_{\alpha 3}$) and of 1.46 (model $DS_{\alpha 4}$).
- a stent thickness s of 0.08 mm (model DS_{s1}) and of 0.06 mm (model DS_{s2});
- a slot length l of 2.92 mm (model DS_{l1}) and of 2.96 mm (model DS_{l2});

The first five columns of Table 1 report the model classification with the corresponding values of the geometrical parameters.

2.1.2. Constitutive material model

The stent is assumed to be made of 316LN stainless steel. The inelastic constitutive response is described through a Von Mises–Hill plasticity model with isotropic hardening. The Young modulus is 196 GPa, the Poisson ratio 0.3, the yield stress 205 MPa (Auricchio et al., 2001).

2.1.3. Mesh sensitivity and simulations

A large deformation analysis is performed using the FEM commercial code ABAQUS (Hibbit Karlsson & Sorenses, Inc., Pawtucket, RI, USA). The FEM was applied to study the stent behavior under internal pressure loading conditions. Due to the circumferential symmetry, only one-twelfth of model DS is discretized by means of eight-node brick elements based on a

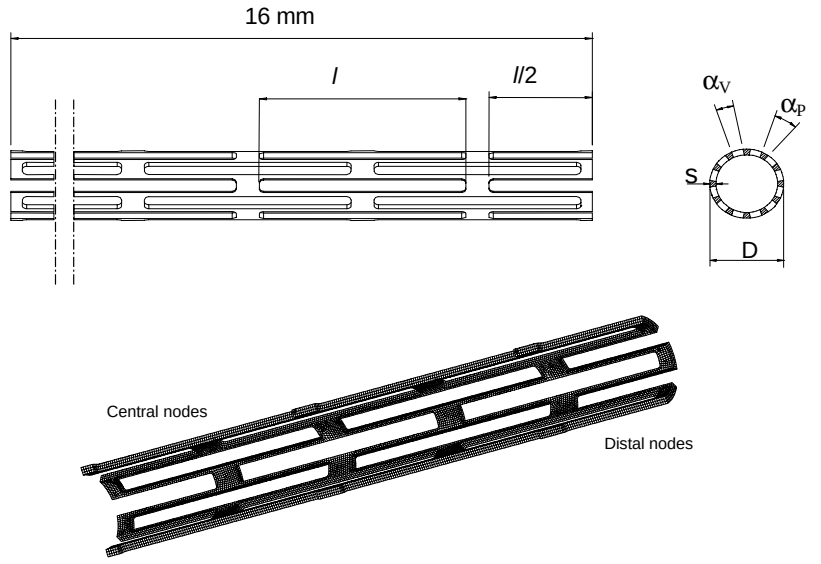

Fig. 1. Geometry of the unexpanded DS stent strut; l: length of the slot, s: thickness, α_P: angle described by the metallic surface, α_V: angle described by the slot and D: outer diameter; finite element mesh for a quarter of model DS stent.

Table 1
Geometric data and results

Model	Design parameters				Results						
	s (mm)	l (mm)	α_P/α_V	m/a	Radial recoil		Long. recoil (%)	Foreshortening (%)	Dogboning (%)	$P_{1.5\,mm}$ (MPa)	PEEQ
					Central (%)	Distal (%)					
DS	0.1	2.88	0.30	0.329	2.90	2.87	−0.66	6.69	27.87	0.283	0.121
$DS_{\alpha 1}$	0.1	2.88	0.20	0.251	3.74	3.40	−0.87	6.27	22.52	0.173	0.108
$DS_{\alpha 2}$	0.1	2.88	0.60	0.438	2.21	2.19	−0.56	7.19	37.11	0.500	0.205
$DS_{\alpha 3}$	0.1	2.88	1.00	0.580	1.82	1.70	−0.60	9.61	59.54	0.740	0.340
$DS_{\alpha 4}$	0.1	2.88	1.46	0.635	1.74	1.53	−0.68	11.97	66.33	0.815	0.400
DS_{mod}	0.1	2.88	0.3/0.6	0.333	2.92	3.95	−0.46	4.08	−46.25	0.306	0.106
DS_{s1}	0.08	2.88	0.30	0.329	2.70	2.63	−0.68	7.21	33.96	0.233	0.164
DS_{s2}	0.06	2.88	0.30	0.329	2.74	2.66	−0.77	8.07	43.94	0.164	0.192
DS_{l1}	0.1	2.92	0.30	0.319	2.99	2.78	−0.69	6.62	28.68	0.289	0.141
DS_{l2}	0.1	2.96	0.30	0.289	3.25	3.08	−0.73	6.41	27.70	0.255	0.123

s: thickness; l: length; m/a: metal-to-artery ratio.

displacement formulation. The presence of a longitudinal symmetry allows to study half of the length; in the following the nodes belonging to the free extremity are referred as *distal*, while those lying on the symmetric plane as *central* (Fig. 1). The meshes were automatically generated by the commercial code GAMBIT (Fluent Inc., Lebanon, NH, USA). In particular, the 10 models of Table 1 were meshed with a total number of brick elements ranged between 2568 and 3840, corresponding to a number of nodes ranged between 4660 and 6560, respectively. As regards the boundary conditions, the nodes belonging to a symmetric plane are required to have zero displacement in the direction normal to the symmetry plane.

Before running the parametric analysis, a sensitivity test was performed to control the influence of the element number on the results. Indeed, model DS was meshed with eight-node brick elements with a number of nodes of 4240, 11,280, and 39,312. The displacements of the central nodes were checked under a radial pressure

of 1 MPa: the percent differences between the finest and the other meshes were of 0.49% and 0.21%, respectively. It is possible to conclude that this problem is not sensitive to the grid refinement of the mesh.

Moreover, since the code GAMBIT has a better performance using tetrahedral elements when the model geometry is complex, a sensitivity test was also performed to control the influence of the element type on the results. Hence, model DS was meshed with 10-node tetrahedral elements. Three meshes with 5567, 7440, 13,341 nodes were compared with the finest brick mesh (39,312 nodes): the percent differences noticed in the central node displacements were 1.78%, 0.95% and 0.40%, respectively. The problem is not sensitive to the grid type, when a number of sufficiently high elements are taken into account.

Simulations were organized in three levels.

Initially, simulations were performed to mimic the free expansion of the stent. A uniform linearly increasing radial pressure (P) was applied at the internal surface of the stent till the radius reached the value of 2 mm in the central region. At this stage the following quantities were calculated:

- the pressure ($P_{2\,\mathrm{mm}}$); and
- the distal radius (R_{distal}).

Then, simulations were performed to investigate the behavior of the stent up to a diameter of 3 mm, which corresponds to a typical inner diameter of a coronary vessel. This means that the stent was loaded by an internal uniform radial pressure up to its reaching 1.5 mm radius in the central region ($R^{\mathrm{load}}_{\mathrm{central}}$). At this stage the following quantities were calculated:

- the pressure ($P_{1.5\,\mathrm{mm}}$);
- the longitudinal length (L^{load}); and
- the distal radius ($R^{\mathrm{load}}_{\mathrm{distal}}$).

Finally, simulations were performed to investigate the mechanical properties of the stent after the load removal. The stent was unloaded decreasing the internal pressure up to zero. At this stage the following quantities were calculated:

- the equivalent plastic strain (PEEQ) evaluated as $\int_0^t \sqrt{\frac{2}{3}\dot{\varepsilon}^{\mathrm{pl}} : \dot{\varepsilon}^{\mathrm{pl}}}\,\mathrm{d}t$, where $\dot{\varepsilon}^{\mathrm{pl}}$ is the increment of the plastic strain tensor;
- the longitudinal length (L^{unload});
- the central radius ($R^{\mathrm{unload}}_{\mathrm{central}}$); and
- the distal radius ($R^{\mathrm{unload}}_{\mathrm{distal}}$).

2.1.4. Output quantities

The result values obtained from the simulations were used to calculate the following quantities:

- the *distal and central radial recoil*, defined as

$$\text{Distal radial recoil} = \frac{R^{\mathrm{load}}_{\mathrm{distal}} - R^{\mathrm{unload}}_{\mathrm{distal}}}{R^{\mathrm{load}}_{\mathrm{distal}}},$$

$$\text{Central radial recoil} = \frac{R^{\mathrm{load}}_{\mathrm{central}} - R^{\mathrm{unload}}_{\mathrm{central}}}{R^{\mathrm{load}}_{\mathrm{central}}},$$

- the *longitudinal recoil*, defined as

$$\text{Longitudinal recoil} = \frac{L^{\mathrm{load}} - L^{\mathrm{unload}}}{L^{\mathrm{load}}},$$

- the *foreshortening*, defined as

$$\text{Foreshortening} = \frac{L - L^{\mathrm{load}}}{L},$$

- the *dogboning*, defined as

$$\text{Dogboning} = \frac{R^{\mathrm{load}}_{\mathrm{distal}} - R^{\mathrm{load}}_{\mathrm{central}}}{R^{\mathrm{load}}_{\mathrm{distal}}}.$$

2.2. Different stent geometries

A new model, model $\mathrm{DS}_{\mathrm{mod}}$, was obtained modifying model DS: the dimension of the 12 circumferential slots in the distal part was reduced, increasing the $\alpha_{\mathrm{P}}/\alpha_{\mathrm{V}}$ ratio from 0.3 to 0.6.

Furthermore, two additional models were considered resembling two stents in use at the moment (Multi-Link Tetra[2] and Carbostent[3]): the principal dimensions (stent length $L = 16$ mm, outer diameter $D = 1.2$ mm and thickness $s = 0.1$ mm) are similar to those adopted for model DS; the material parameters are left unchanged as well. These two models were meshed with 10-node tetrahedral elements. The former (model GEO1, number of nodes equal to 176,584, top of Fig. 2a) has a corrugated ring pattern with a metal-to-artery ratio (m/a) of 0.341. It does not show any longitudinal or circumferential symmetry. The latter (model GEO2, number of nodes equal to 89,918, bottom of Fig. 2b) exhibits a cellular geometry with a metal-to-artery ratio (m/a) of 0.345. Its longitudinal symmetry allows studying only half of the length.

These models were compared with model DS, to investigate the effects of the design on the stent performance.

[2] Guidant, Indianapolis, IN, USA.

[3] Sorin Biomedica, Saluggia, Italy.

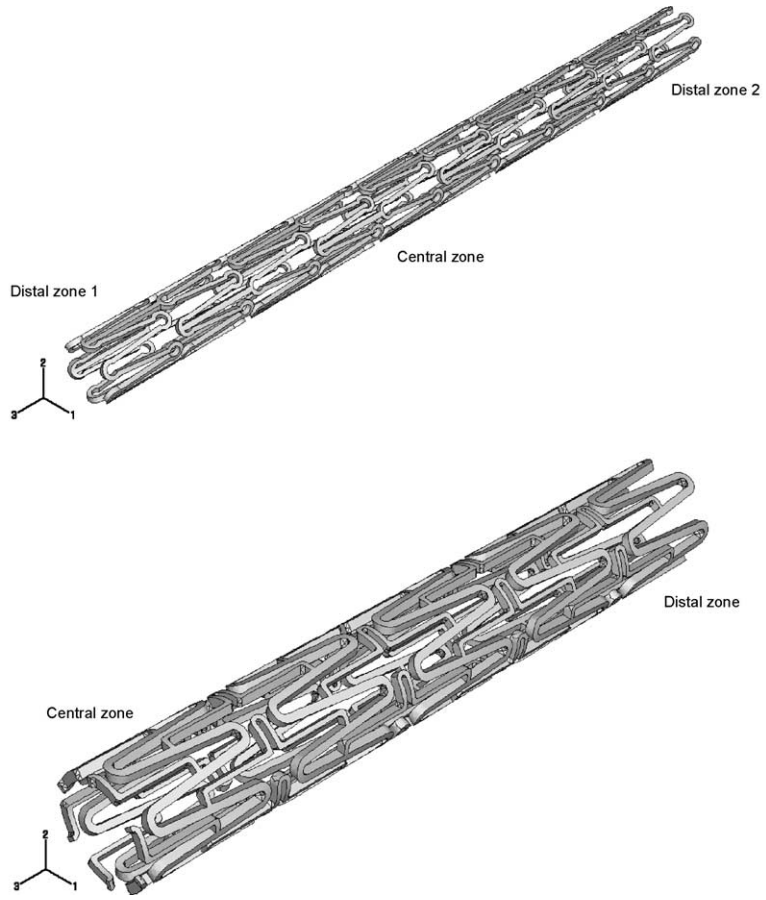

Fig. 2. GEO1 (top) and GEO2 (bottom) models. The former is complete, as there are no geometrical symmetries, while the latter is represented only for a half of its length.

3. Results and discussion

3.1. DS stent

The first series of simulations evinced the strong influence of the metal-to-artery ratio (α_P/α_V) on the pressure increment necessary to expand the stent up to a radius of 2 mm in the central zone (Fig. 3 top). Indeed, in the case of $\alpha_P/\alpha_V = 0.2$, a value of 0.12 MPa is sufficient to expand the stent; an increment of only 0.09 MPa produces a radius of 2 mm very steeply; in the case of $\alpha_P/\alpha_V = 1.46$, 0.57 MPa is necessary to start the expansion and only after an additional increment of 0.34 MPa, the radius expansion is completed (Fig. 3 bottom).

One of the undesirable effects during the stent implant, is the so-called *dogboning*: it consists in a stronger expansion of the distal zone with respect to the central one. Fig. 4 demonstrates the different relevance of this effect in stents having different metal-to-artery ratio. In particular, the dogboning decreases with the α_P/α_V ratio.

Table 1 summarizes the results of the simulations where the stent is loaded till the radius in the central zone reaches 1.5 mm and subsequently it is unloaded. Results are expressed in terms of radial and longitudinal recoil, foreshortening, dogboning, pressure required to reach an expanded stent radius, in the central zone, equal to 1.5 mm ($P_{1.5\,mm}$) and the equivalent plastic strain (PEEQ).

These results show the influence of the geometry on the stent behavior:

- Increasing the ratio α_P/α_V, the radial and longitudinal recoil decrease, while the foreshortening, the dogboning, the pressure $P_{1.5\,mm}$ and the PEEQ increase.
- Decreasing the thickness s, the longitudinal recoil, the foreshortening, the dogboning, and the PEEQ increase, while the pressure $P_{1.5\,mm}$ decreases. The radial recoil does not seem to be significantly influenced by the thickness variation.
- Increasing the slot length l, the radial recoil increases, while the other quantities are not significantly influenced by its variation.

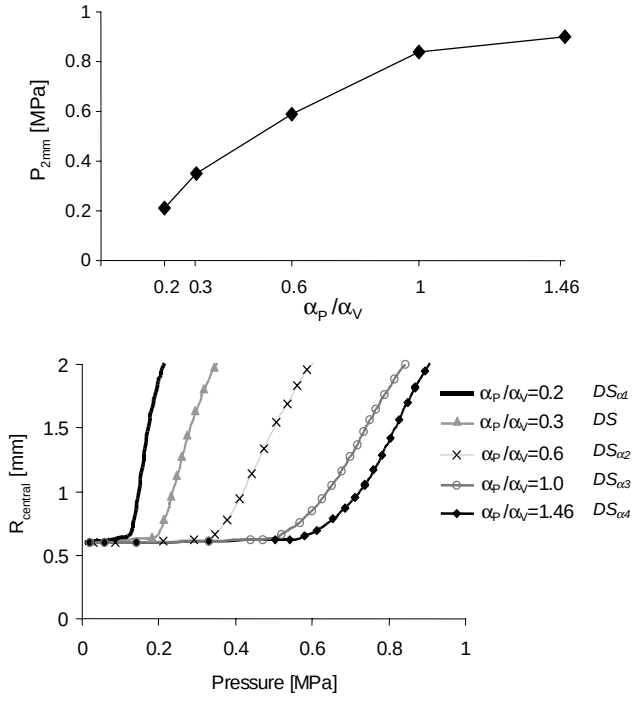

Fig. 3. Top: pressure necessary ($P_{2\,mm}$) to reach a radius equal to 2 mm in the central zone as a function of the metal-to-artery ratio; bottom: central radius as function of the pressure for models with different metal-to-artery ratio.

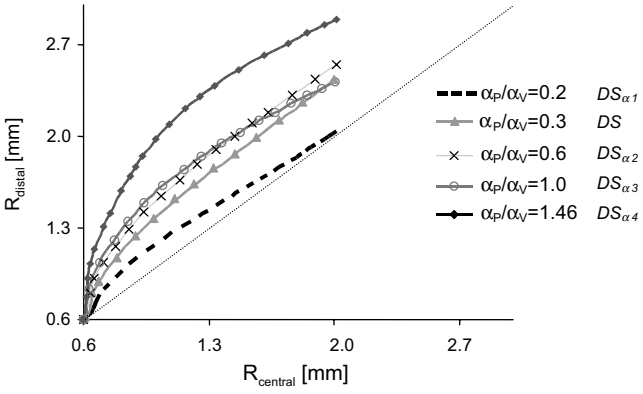

Fig. 4. Expansion of the distal and central radius for the DS stents: reducing the metal-to-artery ratio and increasing the inflation pressure, the expansion tends to become uniform along the stent; dot lines represent the uniform stent expansion.

3.2. Different stent geometries

Fig. 5 shows the Von Mises stress distribution along the stent in the load condition for Models DS, GEO1 and GEO2: as was expected, all the stresses are concentrated in the area of connection between slots; here the development of plastic hinges allows the stent expansion.

Fig. 6 depicts the effects of the different stent geometries on the central and distal radius expansion.

In the modified distal geometry (DS_{mod}), the distal nodes have smaller radial displacement than the central ones (dogboning −46.25%): varying the ratio α_P/α_V, it is possible to control the dogboning effect up to obtain an opposite effect. The value of the pressure necessary to expand the distal zone until an outer radius value of 1.5 mm is higher than that of model DS (0.42 vs. 0.25 MPa), while, as it was expected, the central zone is expanded with a pressure approximately equal (Fig. 6, top).

In model GEO1, the distal expansion has a different behavior according to the orientation of the ring pattern. In 'distal zone 1' (Fig. 2) the expansion is more pronounced than in 'distal zone 2'. In particular, in 'distal zone 1' the dogboning effect is absent, while in 'distal zone 2', an effect opposite to the dogboning is present. This peculiar behavior is due to the particular stent design which shows less metal surface at 'distal zone 2': the net force applied in this area is lower than in the other areas of the stent strut, since the pressure is uniformly applied along the stent surface. As a consequence, the expansion is expected to be smaller. The inclusion of a balloon in the analysis would have certainly mitigated this anomalous behavior. For this reason, the computation of the quantities of interest was performed in both the distal zones. Furthermore, this model shows the lowest pressure necessary to reach an outer radius value of 1.5 mm in 'distal zone 1' (0.31 MPa), while in 'distal zone 2', it has a behavior similar to model DS.

In model GEO2, the central and distal radial expansions are similar and the dogboning effect is nearly absent. The value of pressure necessary to expand the distal zone until an outer radius value of 1.5 mm is similar to that of model DS_{mod} (0.45 MPa).

Finally, model DS_{mod} has a radial recoil comparable with model DS, while model GEO1 does not show any recoil; model GEO2 has a radial recoil similar to model DS, whereas the longitudinal recoil is negligible. As a last remark, it can be noticed that the foreshortening in model DS_{mod} is lower than in model DS, while models GEO1 and GEO2 show higher values (Table 2).

4. Limitations

The modeling of a coronary stent from the implantation until the complete integration in the host artery is a challenging study. Indeed, the implantation involves contact between balloon, stent and diseased artery; the long-term behavior involves interaction between the stent, the artery and the blood flowing through this structure. This study addresses only the free stent expansion. The interaction between the balloon and

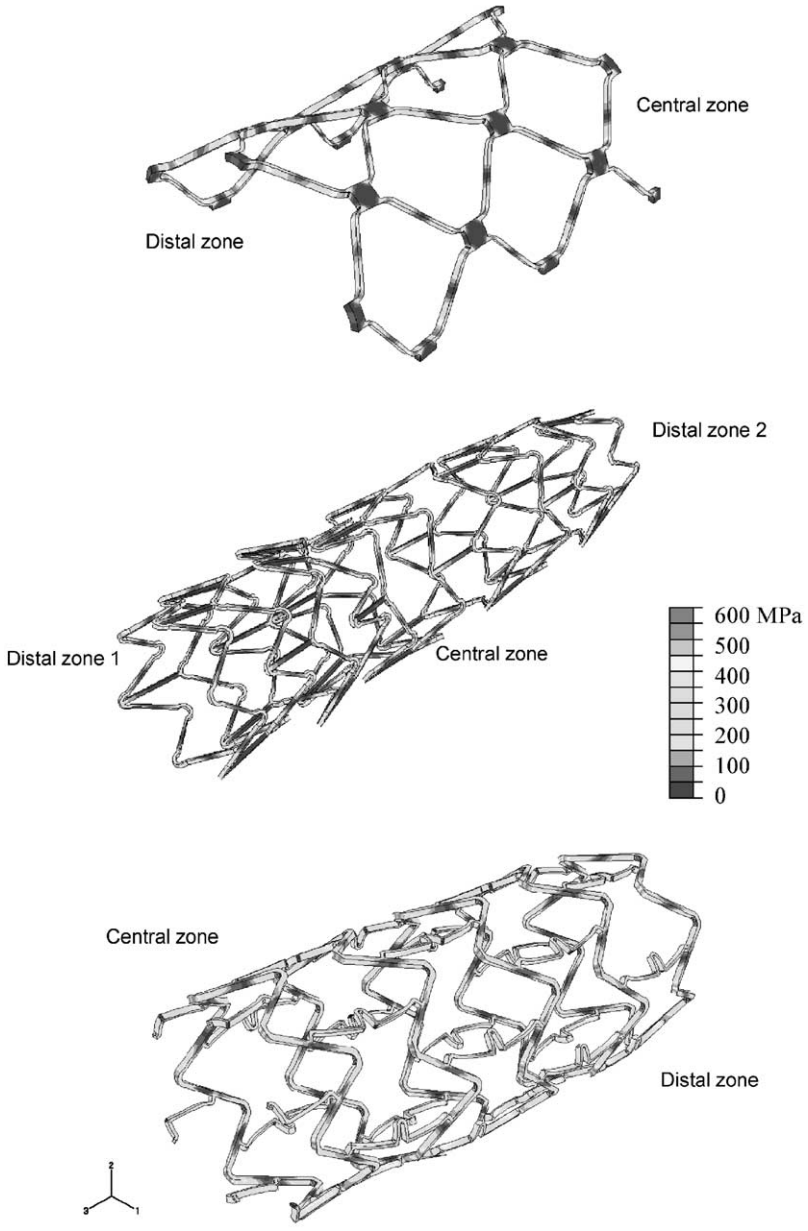

Fig. 5. Von Mises stress contours for models DS, GEO1 and GEO2[4].

the stent has not been modeled, even if the effects of the balloon expansion have been simulated with a uniform pressure, as reported also by Dumoulin and Cochelin (2000), applied directly on the internal metallic surface of the stent through follower loads. Furthermore, the variable thickness strut, which is an important parameter in the optimization of conformability and scaffolding, has not been considered in the present study, although the shape patterns of the stent have been reproduced in detail.

Actually, the analysis of the stent mechanical behavior would require an appropriate modeling of arterial vessel and atherosclerotic plaque and the simulation of their contact with the stent: these features will be evaluated in future studies.

5. Conclusions

A finite element analysis similar to the one herewith proposed could help in designing new stents or analyzing actual stents to ensure ideal expansion and

[4]A colour version of this figure can be found at http://wwwlabs.stru.polimi.it/downloads

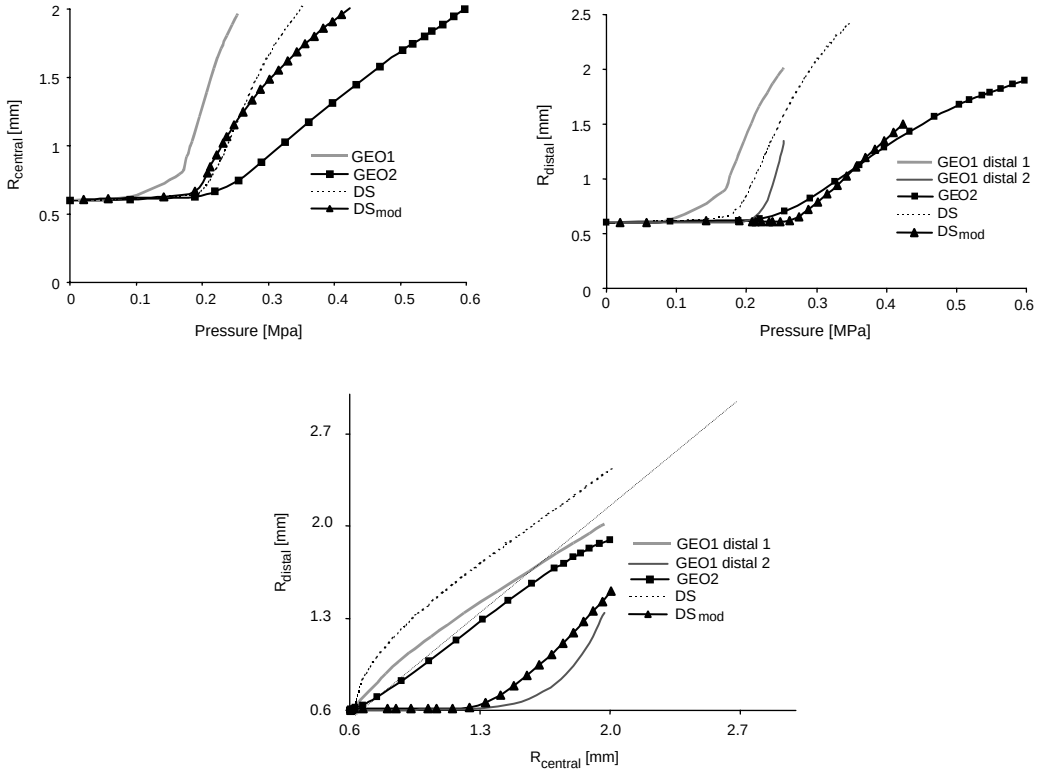

Fig. 6. Comparison of the central and distal radius expansion at different values of internal pressure (top) and comparison between distal and central radius (bottom) for models DS, DS_{mod}, GEO1 and GEO2; dot lines as in Fig. 4.

Table 2
Results for the two different stent geometries

Model	Design parameters		Results											
	s (mm)	m/a	Radial recoil (%)			Long. recoil (%)		Foreshortening (%)		Dogboning (%)		$P_{1.5\,mm}$ (MPa)	PEEQ
			Central	Distal zone 1	Distal zone 2	Distal zone 1	Distal zone 2	Distal zone 1	Distal zone 2	Distal zone 1	Distal zone 2		
GEO1	0.1	0.341	0.26	0.29	0.64	−0.01	−0.01	13.61	8.25	−0.18	−56.44	0.215	0.202
GEO2	0.1	0.345	2.17	1.68		−0.06		9.75		−2.30		0.446	0.378

s: thickness; m/a: metal-to-artery ratio.

structural integrity, substituting in vitro experiments often difficult and unpractical.

These results are promising and useful in the study of the mechanical performances of the stent itself. In particular, they pointed out the possibility to optimize the radial expansion of the classical stent by varying the α_P/α_V ratio along the stent or only in the distal part or changing the stent pattern shape.

Acknowledgements

The partial support of the National Research Council (CNR) grant Agenzia2000 is duly acknowledged.

References

Auricchio, F., Di Loreto, M., Sacco, E., 2001. Finite-element analysis of a stenotic artery revascularization through a stent insertion. Computer Methods in Biomechanics and Biomedical Engineering 4, 249–263.

Barragan, P., Rieu, R., Garitey, V., Roquebert, P.-O., Sainsous, J., Silvestri, M., Bayet, G., 2000. Elastic recoil of coronary stents: a comparative analysis. Catheterization and Cardiovascular Interventions 50, 112–119.

Bjarnason, H., Hunter, D.W., Crain, M.R., Ferral, H., Miltz-Miller, S.E., Wegryn, S.A., 1993. Collapse of a Palmaz stent in the subclavian vein. American Journal of Roentgenology 160, 1123–1124.

Dangas, G., Fuster, V., 1996. Management of restenosis after coronary intervention. American Heart Journal 132, 428–436.

Dotter, C.T., 1969. Transluminally placed coil spring end arterial tube grafts, long-term patency in canine popliteal artery. Investigative Radiology 4, 329–332.

Dumoulin, C., Cochelin, B., 2000. Mechanical behaviour modelling of balloon-expandable stents. Journal of Biomechanics 33, 1461–1470.

Dyet, J.F., Watts, W.G., Ettles, D.F., Nicholson, A.A., 2000. Mechanical properties of metallic stents: how do these properties influence the choice of stent for specific lesions? Cardiovascular and Interventional Radiology 23, 47–54.

Etave, F., Finet, G., Boivin, M., Boyer, J.-C., Rioufol, G., Thollet, G., 2001. Mechanical properties of coronary stents determined by using finite element analysis. Journal of Biomechanics 34, 1065–1075.

Fabregues, S., Baijens, K., Rieu, R., Bergeron, P., 1998. Hemodynamics of endovascular prostheses. Journal of Biomechanics 31, 45–54.

Fischman, D.L., Leon, M.B., Baim, D.S., Schatz, R.A., Savage, M.P., Penn, I., Detre, K., Veltri, L., Ricci, D., Nobuyoshi, M., et al., 1994. A randomized comparison of coronary-stent placement and balloon angioplasty in the treatment of coronary artery disease. Stent restenosis study investigators. The New England Journal of Medicine 331, 496–501.

Gottsauner-Wolf, M., Moliterno, D.J., Lincoff, A.M., Topol, E.J., 1996. Restenosis—an open file. Clinical Cardiology 19, 347–356.

Oh, S., Kleinberger, M., McElhaney, J.H., 1994. Finite-element analysis of balloon angioplasty. Medical and Biological Engineering and Computing 32, S108–S114.

Ormiston, J.A., Dixon, S.R., Webster, M.W.I., Ruygrok, P.N., Stewart, J.T., Minchington, I., West, T., 2000. Stent longitudinal flexibility: a comparison of 13 stent designs before and after balloon expansion. Catheterization and Cardiovascular Interventions 50, 120–124.

Peacock, J., Hankins, S., Jones, T., Lutz, R., 1995. Flow instabilities induced by coronary artery stents: assessment with an in vitro pulse duplicator. Journal of Biomechanics 28, 17–26.

Rieu, R., Barragan, P., Masson, C., Fuseri, J., Garitey, V., Silvestri, M., Roquebert, P., Sainsous, J., 1999. Radial force of coronary stents: a comparative analysis. Catheterization and Cardiovascular Interventions 46, 380–391.

Rogers, C., Tseng, D.Y., Squere, J.C., Edelman, E.R., 1999. Balloon-artery interactions during stent placement. A finite element analysis approach to pressure, compliance, and stent design as contributors to vascular injury. Circulation Research 84, 378–383.

Rosenfield, K., Schainfeld, R., Pieczek, A., Haley, L., Isner, J.M., 1997. Restenosis of endovascular stents from stent compression. Journal of American College of Cardiology 29, 328–338.

Serruys, P.W., de Jaegere, P., Kiemeneij, F., Macaya, C., Rutsch, W., Heyndrickx, G., Emanuelsson, H., Marco, J., Legrand, V., Materne, P., et al., 1994. A comparison of balloon-expandable-stent implantation with balloon angioplasty in patients with coronary artery disease. Benestent study group. The New England Journal of Medicine 331, 489–495.

Versaci, F., Gaspardone, A., Tomai, F., Crea, F., Chiariello, L., Gioffrè, P.A., 1997. A comparison of coronary-artery stenting with angioplasty for isolated stenosis of the proximal left anterior descending coronary artery. The New England Journal of Medicine 336, 817–822.

Whitcher, F.D., 1997. Simulation of in vivo loading conditions of Nitinol vascular stent structures. Computers and Structures 64, 1005–1011.

Wong, P., Leung, W.H., Wong, C.M., 1996. Migration of the AVE micro coronary stent. Catheterization and Cardiovascular Diagnosis 38, 267–273.